PARAMETRICALLY EXICITED MEMS-BASED FILTERS

Steven W. Shaw[1], Kimberly L. Turner[2], Jeffrey F. Rhoads[1], and Rajashree Baskaran[2]

[1]Department of Mechanical Engineering, Michigan State University; [2]Department of Mechanical and Environmental Engineering, University of California - Santa Barbara

Abstract: In this paper we describe the dynamics of MEMS oscillators that can be used as frequency filters. The unique feature of these devices is that they use parametric resonance, as opposed to the usual linear resonance, for frequency selection. However, their response in the parametric resonance zone has some undesirable features from the standpoint of filter performance, most notably that their bandwidth depends on the amplitude of the input and the nonlinear nature of the response. Here we provide a brief background on filters, a MEMS oscillator that overcomes some of the deficiencies, and we offer a description of how one might utilize a pair of these MEMS oscillators to build a band-pass filter with nearly ideal stopband rejection. These designs are made possible by the fact that MEMS devices are highly tunable, which allows one to build in system features to achieve desired performance.

Key words: MEMS, Parametric Resonance, Filters

1. INTRODUCTION

As the demand for wireless communications technology continues to increase, so too does the demand for effective and efficient band-pass filters, as these devices, which pass signals with frequency components inside a specific bandwidth while attenuating those outside of it, are often integral components of such technology. While much research has been done on the design and performance of conventional electrical band-pass filters (for example, [1]), and their mechanical analogs (for example, [2]), the aforementioned demand for increased performance has led to a search for other alternatives. One that has shown early promise is to create

microelectromechanical systems (MEMS) filters [3]. These micro-scale components are more desirable than their more conventional counterparts primarily due to their size, low power consumption, and ease of integration with electrical systems. Equally important is the fact that MEMS filters have been shown to exhibit quality (Q) factors as high as 80,000 (as reported in [4]). More relevant to the present work are the inherent parametric resonances that occur in certain types of MEMS, which are shown here to be potentially advantageous in filtering applications.

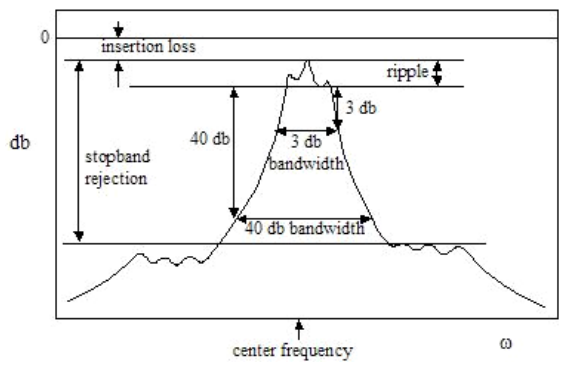

Figure 1. Key Features of the Transmission Frequency Response of a Band-pass Filter. (Adapted from [4])

2. FILTER BASICS

Here we highlight the key features to consider when designing a band-pass filter. Ideally, one would like a device that transmits a harmonic signal essentially intact if its frequency is in a prescribed bandwidth, and completely attenuates the signal if it is outside of the bandwidth. Virtually all filter designs make use of a chain of linear resonators, either electrical [1] or mechanical [2]. Figure 1 depicts a sample frequency response transmission function for such a filter, where the following features are noted:

– The center frequency of the passband.
– The bandwidth of the passband – the range of frequencies to be passed through the filter.
– The stopband attenuation – the amount by which the signal is reduced outside of the passband.

– The insertion loss – the drop-off in signal amplitude as it passes through the filter.
– The sharpness of the roll-off – the width of the frequency range between the edges of the passband and the stopband.
– The flatness of the passband response, which typically has ripples.

3. PARAMETRIC RESONANCE FOR FILTERING

As previously mentioned, one of the interesting features of MEMS oscillators is that, when driven by non-interdigitated comb drives, such as those shown in Figure 2, they exhibit parametric resonances [5]. The existence of such resonances can be traced to the fact that the electrostatic driving and restoring forces acting on such a device result in a fluctuating effective stiffness. While the parametric instability caused by such fluctuations may be undesirable in many applications, the nearly instantaneous jumps that occur in the response amplitude when the parametric resonance is activated may prove to be highly beneficial for filtering, since they result in *nearly ideal stopband rejection* as well as an *extremely sharp response roll-off* outside of the resonance zone. Of course, the use of parametric instability for filtering is not without difficulties. Among the most obvious drawbacks are:
– The bandwidth depends on the excitation amplitude.
– There can exist non-trivial responses outside of the passband.
– There is a nonlinear input/output relationship.
– Higher order resonances may occur.

Fortunately, by employing a novel tuning scheme in conjunction with a specific logic implementation, the effects of most of these drawbacks can be largely overcome. We begin by describing the tuning for a single MEMS oscillator, and then turn to a design that makes use of two such devices.

4. ANALYSIS OF A SINGLE MEMS OSCILLATOR

In an attempt to gain a better understanding of the benefits and drawbacks of a parametrically excited MEMS band-pass filter, as well as how the drawbacks can be overcome, consider the response of a single DOF MEMS oscillator, such as the one depicted in Figure 2. This device consists of a backbone (essentially, the mass) suspended by folded beam springs which is activated by a pair of non-interdigitated comb drives, very similar to the devices considered in [6], [7] and [8].

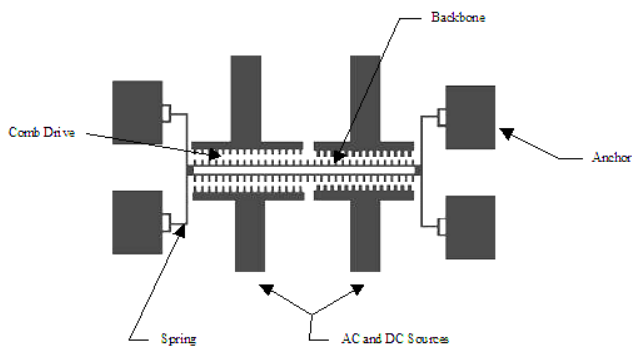

Figure 2. CAD Drawing of a Parametrically Excited MEMS Filter Device.

The equation of motion for this device can be expressed as [7]:

$$m\ddot{x} + c\dot{x} + F_r(x) + F_{es}(x,t) = 0 .$$

The elastic restoring force can be accurately modeled by a cubic function $F_r(x) = k_1 x + k_3 x^3$, where typically the system is mechanically hardening ($k_3 > 0$). The electrostatic driving and restoring forces are assumed to be generated by two separate, essentially frictionless, non-interdigitated comb drives, one providing a DC input voltage V_0 and the other driven by a square-rooted AC signal of amplitude V_A. Again, cubic functions in displacement, proportional to the square of the applied voltage, provide an accurate model [7]:

$$F_{es}(x,t) = \left(r_{10}x + r_{30}x^3\right)V_0^2 + \left(r_{1A}x + r_{3A}x^3\right)V_A^2\left(1 + \cos(\omega t)\right).$$

Note that one can design combs such that any combination of signs on the r coefficients is possible (although their magnitudes are limited). Time is rescaled according to $\tau = \omega_0 t$, where $\omega_0 = (k_1/m)^{1/2}$, and the displacement is rescaled by a characteristic displacement, x_0, (for example, the length of the oscillator backbone), such that $\varepsilon^{1/2} z = x/x_0$, where ε is a scaling parameter introduced for the analysis. The result is a non-dimensional equation of motion for the oscillator of the form

$$z'' + 2\varepsilon\zeta z' + z\left(1 + \varepsilon\nu_1 + \varepsilon\lambda_1\cos(\Omega\tau)\right) + \varepsilon z^3\left(\chi + \nu_3 + \lambda_3\cos(\Omega\tau)\right) = 0$$

where $(\bullet)'$ denotes $d(\bullet)/d\tau$ and the nondimensional parameters are defined in a manner consistent with the above scaling. With this non-dimensional

equation, the oscillator's response can be examined as system parameters and inputs are varied. For example, the parametric resonance instability zone that exists in the V_A versus Ω parameter space is shown in Figure 3 (it is the boundary designated by $\rho = 0$) as created using both perturbation analysis (described below) and simulations.

As Figure 3 shows, the instability zone that exists for this particular oscillator is a 'wedge of instability' with its apex centered at a non-dimensional frequency of 2. In this case, the zero response is stable 'outside' of the wedge, while 'inside' of the wedge the trivial response is unstable, thereby leading to a non-zero response amplitude that is determined by the system nonlinearity. Of course, the response outside of the wedge may be zero or non-zero, depending on the damping, whether the system is hardening or softening, and on initial conditions. Another important feature to note here is that the frequency at which the filtering takes place is at *twice* the natural frequency of the device, and therefore one gets double the filter frequency as compared with using the same device as a filter using direct excitation. We now turn to addressing the amplitude dependent nature of the bandwidth.

5. TUNING FOR CONSTANT FREQUENCY INSTABILITY

As shown, the frequency at which the oscillator is activated depends on the amplitude of the alternating voltage. However, this can be overcome by employing the following tuning scheme, wherein the natural frequency of the oscillator is made to depend on the amplitude of the excitation, by varying the linear electrostatic stiffness. To begin, a proportionality constant, α, is defined that relates the DC voltage input to the AC voltage amplitude, such that $V_0 = \alpha V_A$, which results in a linear electrostatic stiffness that depends on α, the r_1's, k_1, and the input voltage V_A. Substituting this, as well as the other redefined coefficients, back into the non-dimensional equation of motion results in a modified equation of motion for the oscillator,

$$z'' + z = -\varepsilon\left(2\varsigma z' + zA\left(\rho + \cos(\Omega t)\right) + z^3\left(\chi + \nu_3 + \lambda_3 \cos(\Omega \tau)\right)\right)$$

where the linear excitation amplitude is redefined such that $A = \lambda_1$ and a new tuning parameter ρ is introduced which relates the effective electrostatic linear stiffness to the amplitude of excitation. It is related to the designer-selected parameters via,

$$\rho = \frac{\nu_1}{\lambda_1} = 1 + \frac{r_{10}\alpha^2}{r_{1A}} .$$

This parameter allows for the distortion of the instability zone, by changing the linear natural frequency $\omega_n = (1+\varepsilon\rho A)^{1/2}$ in a manner that depends on A. The result of this tuning is a rotation of the wedge of instability; see Figure 3. In particular, for $\rho > 0$ the wedge rotates clockwise and for $\rho < 0$ it rotates counterclockwise. Also, perturbation theory and simulations, created using design parameters similar to those in [6-8], have verified that by selecting $\rho = 1/2$ the left stability boundary becomes essentially vertical, as shown in Figure 3, and, similarly, by selecting $\rho = -1/2$ the right stability boundary becomes essentially vertical.

The $\rho = 1/2$ case makes the oscillator behave like a high pass switch, while the $\rho = -1/2$ case constitutes a low pass switch. However, one must take into account the nonlinear nature of the response, and the fact that there may exist nontrivial responses outside of the instability zone. Also, the response, once activated, may not exist for all frequencies above or below the desired switch frequency. These issues, which depend on the system nonlinearities, are considered subsequently. Also note that the presence of damping creates a threshold voltage level above which the device will function, due to the parametric instability. This is not a major concern here, though, since the damping levels of these devices are anticipated to be very low (with Q's in the thousands). The main point here is that this tuning capability makes it theoretically possible to create amplitude independent switches over a reasonable range of input voltages.

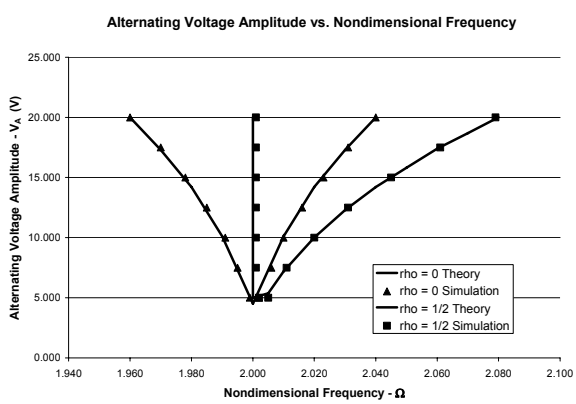

Figure 3. Region of Parametric Instability in the A - Ω Parameter Space; $\rho = 0$ and $\rho = 1/2$.

6. TUNING THE NONLINEARITY

Another desirable feature of MEMS devices is that one can tune the system nonlinearity using the nonlinear nature of the electrostatic forces exerted by the comb drives [6, 7]. This is crucial for achieving the desired behavior of non-trivial solutions outside of the passband. Specifically, the cubic nonlinearity of each oscillator can be specified, and it is desired that the high pass oscillator (with $\rho = 1/2$) have a hardening behavior, so that no nontrivial responses exist below the switch frequency. Similarly, the low pass oscillator (with $\rho = -1/2$) should have softening behavior. In order to consider these responses, we turn to the equations of motion and examine the response using a perturbation method.

The system's averaged equations are given by

$$a' = \frac{1}{8} a\varepsilon\left[-8\varsigma + \left(2A + a^2\lambda_3\right)\sin(2\psi)\right]$$
$$\psi' = \frac{1}{8}\varepsilon\left[3a^2\left(\chi + \nu_3\right) + 4A\rho - 4\sigma + 2\left(A + a^2\lambda_3\right)\cos(2\psi)\right]$$

where a is the response amplitude of the averaged solution, ψ is the phase of the averaged solution, and σ is a detuning parameter defined such that $\Omega_0 = 2+\varepsilon\sigma$. Note that the form of these equations is not the typical nonlinear Mathieu equation, due to the presence of the parametric excitation that acts on the nonlinearity, which affects the nature of the nonlinear responses. Using these equations the theoretical instability curves shown in Figure 3 were generated. Likewise, these equations can be solved to produce approximate analytical response curves, examples of which are shown in Figure 4 for a $\rho = 1/2$ oscillator with a hardening nonlinearity. Simulation data is also shown, verifying the accuracy of the response predictions, which is especially good at low input voltages. The key feature here is that the system behaves like a high pass filter with a very sharp transition at a frequency that is independent of the input voltage amplitude. Note that no secondary instabilities that would lead to more complicated dynamics, such as chaos, are predicted by analysis or seen in simulations. If this occurred, an upper bound on the input voltage may need to be imposed. In addition, it should be noted that any difficulties that may arise due to the overlapping of the nontrivial response branch and a stable trivial solution are negated through the logic implementation described below.

As shown in previous works [6-8] the aforementioned nonlinear tuning can be accomplished by varying the oscillator's cubic electrostatic stiffness. In the proposed design this may be done in a couple of ways: by altering the AC/DC voltage relationship (although the parameter α is used here to set the

value of ρ, and thus another set of combs may be required), or by selective design of the combs to achieve the desired values for the nonlinear electrostatic coefficients (r_{3O} and r_{3A}). These are current research topics under consideration.

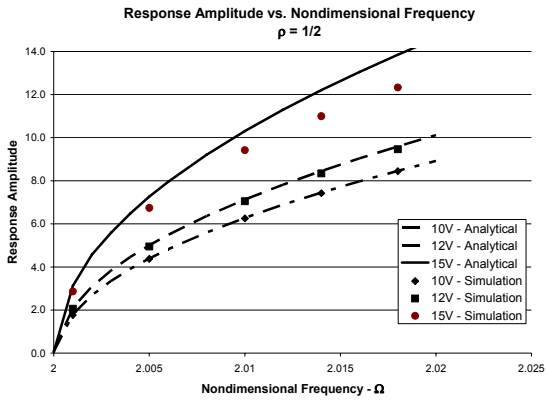

Figure 4. Sample Response Curves – Amplitude vs. Frequency.

7. COMBINING TWO OSCILLATORS INTO A BAND-PASS FILTER

A possible implementation scheme for a band-pass filter is represented in Figure 5. In this system, the idea is to generate a band-pass filter with a center frequency of Ω_0 and a bandwidth of $\Delta\Omega_0$, where Δ represents a small number that prescribes the bandwidth to a percentage of the center frequency. To accomplish this, two oscillators, which are ideally isolated to avoid internal resonances, are employed, one with $\rho = 1/2$ and a hardening nonlinearity, which will be designated as 'H', for high pass, and another with $\rho = -1/2$ and a softening nonlinearity, which will be designated as 'L', for low pass. To develop the specified bandwidth in the final system, these oscillators must be specially tuned so that the apexes of each of the respective wedges are slightly shifted. Specifically, the zero-voltage linear frequencies are designed such that the H oscillator's frequency is $\Delta\Omega_0/2$ below the center frequency and L's is $\Delta\Omega_0/2$ above it.

We now take the two oscillators, tuned using the electrostatic linear and nonlinear tunings described previously, and also tune their zero-voltage frequencies as described immediately above, so that the desired 'H' and 'L'

characteristics are achieved. These are then incorporated into a MEMS with the logic indicated in Figure 5 below.

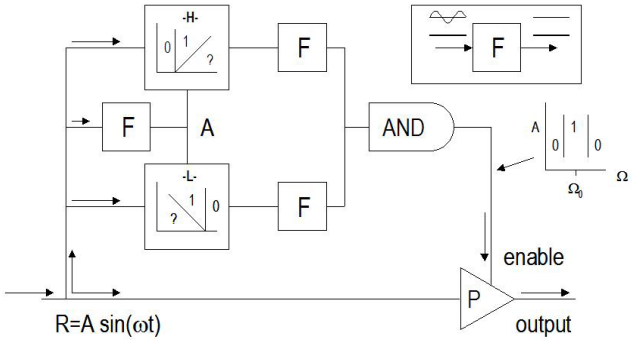

Figure 5. Hardware Implementation Scheme.

This filter system is designed to work as follows. A harmonic signal R is input into the system. This input is used to drive the two oscillators, and, in addition, its amplitude A is determined using block F (an AC to DC converter). A is used as an input to tune the oscillators through the parameters $\rho = \pm 1/2$. The oscillators are designated by blocks H and L, each of which shows a simple logic diagram in A - Ω space, showing 0 where the response must be trivial, 1 where it must be nontrivial, and ? where it may be either, depending on parameters and initial conditions. After each oscillator does its respective filtering, its output is sent to another block F which converts the output signal into a constant voltage, say unity or zero, depending on the results of the filtering. The two resulting voltages are then fed into an AND block which produces a zero voltage unless the frequency is in the desired passband. The output of the AND block provides a signal to an enabling device P which allows the signal to pass only if it sees a nonzero enabling signal. The amplitude dependent linear tuning makes the edges of the stopbands independent of the voltage amplitude (above a certain small threshold), and the nonlinear tuning and the logic ensure that the output of the AND gate is as desired. This produces a MEMS filter with ideal stopband rejection and essentially infinitely sharp roll-off characteristics.

8. CONCLUSION

This paper outlines a means of achieving a band-pass filter using parametric resonance in MEMS. The main features of the system are achieved through the highly tunable nature of these devices. However, several topics remain to be resolved for the final realization of such a filter.

First, the input/output relationship for parametric resonance is nonlinear; while the logic shown in Figure 5 may overcome this obstacle, simpler logic may be possible if one can somehow 'linearize' this relationship. Also, the existence of higher order parametric resonances remains an issue [5], although this issue may be addressed by specifying the damping level such that they do not occur over operational ranges of voltage. In addition, the insertion loss of such a device must be considered to ensure that the overall signal drop-off is acceptable. Finally, since the input considered here is idealized, future works will need to consider more realistic inputs, including those which feature noise. The implementation of the linear and nonlinear tuning described herein in an actual device is currently underway. The ultimate goal is, of course, the integration of the two MEMS oscillators, with the described tuning features, and the logic of Figure 5 onto a single filter chip.

ACKNOWLEDGEMENTS

This work is supported by the AFOSR under contract F49620-02-1-0069.

REFERENCES

1. Taylor, J.T., and Q. Huang. (eds.), *CRC Handbook of Electrical Filters*, CRC Press, Boca Raton, 1997.
2. Johnson, R.A., Borner, M., and M. Konno, "Mechanical Filters – A Review of Progress," *IEEE Transactions of Sonics and Ultrasonics,* SU-18, 3, 1971.
3. Nguyen, C.T.-C., "Micromechanical Filters for Miniaturized Low-Power Communications," *Proceedings of SPIE*: Smart Structures and Materials (Smart Electronics and MEMS), Newport Beach, California, March 1-5, 1999.
4. Wang, K. and C.T.-C. Nguyen, "High-Order Micromechanical Electronic Filters," *Proceedings, 1997 IEEE International Micro Electro Mechanical Workshop*, Nagoya, Japan, 25-30.
5. Turner, K.L., Miller, S.A., Hartwell, P.G., MacDonald, N.C., Strogatz, S.H., and S.G. Adams, "Five Parametric Resonances in a Microelectromechanical System," *Nature*, 396, 149-152, 1998.
6. Adams, S.G., Bertsch, F., and N.C. MacDonald, "Independent Tuning of Linear and Nonlinear Stiffness Coefficients," *Journal of Microelectromechanical Systems,* 7 (2), 172-180, 1998.
7. Zhang W., Baskaran R., and K.L. Turner, "Effect of Cubic Nonlinearity on Auto-parametrically Excited MEMS Mass Sensor," *Sensors & Actuators A*, 3758, 2002.
8. Zhang W., Baskaran R., and K.L. Turner, "Tuning the Dynamic Behavior of Parametric Resonance in a Micro Mechanical Oscillator", *Applied Physics Letters*, 82, 130, 2003.